

Nagaoka Ferromagnetism in 3×3 Arrays and Beyond

Yan Li,^{1,*} Keyi Liu,¹ and Garnett W. Bryant^{1,2}

¹*Joint Quantum Institute,*

University of Maryland and National Institute of Standards and Technology, College Park, Maryland 20742, USA

²*Nanoscale Device Characterization Division,*

National Institute of Standards and Technology, Gaithersburg, Maryland 20899, USA

(Dated: April 8, 2024)

Nagaoka ferromagnetism (NF) is a long-predicted example of itinerant ferromagnetism (IF) in the Hubbard model that has been studied theoretically for many years. The condition for NF, an infinite onsite Coulomb repulsion and a single hole in a half-filled band, does not arise naturally in materials, and was only realized recently for the first time in experiments on a 2×2 array of gated quantum dots. Atomically precise fabrication of dopant arrays in Si allows for engineering highly controllable systems with complex geometries. This makes dopant arrays a good candidate to study NF in different array geometries through analog quantum simulation. Here we present theoretical simulations done for 3×3 arrays and larger $N \times N$ arrays of quantum dots, and predict the emergence of different forms of ferromagnetism in different geometries. We find NF in perfect 3×3 arrays, as well as in $N \times N$ arrays for one hole less than half-filling. The ratio of the Hubbard on-site repulsion U to hopping t that defines the onset of NF increases as N increases, approaching the bulk limit of infinite U for large N . Additional simulations are done for geometries made by removing sites from $N \times N$ arrays. Different forms of ferromagnetism are found for different geometries. Loops show ferromagnetism, but only for three electrons. For loops, the critical U/t for the onset of ferromagnetism decreases as the loop length increases. We show that this different dependence on size for loops and $N \times N$ arrays can be understood by a scaling argument. Our results show how analog quantum simulation with small arrays can elucidate the role of effects including wavefunction connectivity; system geometry, size and symmetry; bulk and edge sites; and kinetic energy in determining the quantum magnetism of small systems.

I. INTRODUCTION

Nagaoka ferromagnetism (NF) is a well-known result of the Hubbard model, where Nagaoka [1] proved rigorously the existence and uniqueness of a saturated, ferromagnetic ground state in a single-band Hubbard model on a lattice. In the case of one hole in a half-filled band and infinite, repulsive, same-site Coulomb interaction U between opposite spins, the ground state has the maximum total spin S . This comes from a non-trivial interplay between quantum dynamics and Coulomb interaction, where the kinetic and repulsive energy terms compete resulting in a ferromagnetic ground state. This competition is determined by how the single hole can move around the lattice.

NF is one of the exact results for itinerant ferromagnetism (IF) and has been studied theoretically for years in various conditions [2, 3]. However, the specific conditions proved by Nagaoka do not arise in any natural materials and has only been observed experimentally for the first time in an engineered 2×2 quantum dot plaquette [4]. It remains an open question when NF can be extended to larger, finite-systems that have internal as well as edge sites, how NF would behave in realistic conditions where U is large but not infinite, and how NF is affected by long-range interactions or disorder.

Following Nagaoka's original work, many have tried to

generalize Nagaoka's result. Tasaki provided a proof of a generalized version of Nagaoka's theorem [2]. Mielke and others found a new class of ferromagnetism states in the Hubbard Model which they called "flat-band ferromagnetism" [5]. The possibility of extending NF to finite U with finite densities of holes has also been studied for different infinite lattices [6, 7]. There have also been many theoretical works done on the instability of NF, that show when NF does not take place [8–10].

In recent years, as computational techniques have advanced, there has been more discussion of small, finite systems that exhibit NF. For example, finite lattices with up to 24 sites with periodic boundary conditions were studied using quantum Monte Carlo [11, 12]. Different geometries of finite systems were studied using exact diagonalization techniques (ED) [13, 14]. These studies revealed the importance of geometry for realizing NF in finite systems, which could be achievable with current experiments using gated quantum dot or dopant arrays.

Quantum dots, also known as artificial atoms, can be used as quantum simulators which can perform simulations beyond what classical computers can do [15–18]. Among various experimental platforms, dopant-based quantum dots have many advantages, such as the precise placement of dopant atoms and tunable site-to-site hopping amplitude, making them a strong candidate for simulating strongly correlated systems, like the Hubbard Model in the large U limit. Silver recently fabricated 3×3 arrays of single/few-dopant quantum dots and demonstrated analog quantum simulation of a 2D Fermi-Hubbard Model with tunable parameters [19]. This pro-

* yan.li@nist.gov

vides an experimental pathway to probe the NF in 3×3 arrays and in many other finite geometries.

In this paper, we use ED to simulate 3×3 dopant arrays in the conditions required for NF, i.e. one less electron than a half filled band and in the large U limit. We predict that NF will exist in a 3×3 array, as in a 2×2 array, as well as in $N \times N$ arrays, for a finite region of t/U , where t is the nearest-neighbor hopping. For t/U below the transition point, the ground state of the system has maximum total spin S , i.e. the ground state is ferromagnetic. Since the direction of the ferromagnetism is arbitrary, the system's energy only depends on total spin S but not the spin in the z -direction (s_z). The ferromagnetic state with maximum $s_z = S$ with all of the spins aligned in the same z direction is degenerate with all other ferromagnetic states with smaller s_z as long as they have the same total S . The ground state is $(2S+1)$ -fold degenerate when there is Nagaoka ferromagnetism. Above the transition point, the ground state is no longer the maximum total spin state and is no longer ferromagnetic. We simulate variations of the perfect 3×3 array to determine when NF is robust to experimental impurities or disorder.

The quantum nature of magnetism plays an essential role in determining how and when magnetism occurs. The small-scale simulators that we consider in this paper provide an excellent testbed for investigating quantum effects. We find that the connectivity of the many-body wavefunction plays a key role in determining when NF can occur or when other forms of itinerant ferromagnetism at fillings other than one hole in a half-filled band, that is, rather than NF, can occur. Band filling is another key condition that determines the type of ferromagnetism. We will show that very different fillings, related to the number of holes in a half-filled band or the number of electrons in an empty band will define the possibility of ferromagnetism in similar, related structures. The competition between kinetic energy and coulomb repulsion determines where in t/U space the transition to ferromagnetism occurs. The t/U ratio at the transition can increase or decrease with system size, depending on the array geometry (and the related wavefunction connectivity), and the band filling. We develop a simple scaling argument to explain both types of size-dependence and the critical role that the kinetic energy plays, through its dependence on band filling, in determining the form of the scaling. The role of these quantum effects will be highlighted as we discuss NF in different small arrays to show how quantum simulation with small arrays could reveal these critical effects. It should be emphasized that dopant arrays, once they can be made perfectly [20] would be an versatile solid-state platform to explore the diversity of arrays and the range of effects that we discuss.

The paper is structured as follows: In Section II, we discuss the 2D Hubbard Model, the signatures of finding NF in finite systems, and how the systems are modelled in our simulations. In Section III, we present our sim-

ulation results for the 3×3 and $N \times N$ square arrays, which exhibit NF up to a finite t/U transition point that decreases with increasing N . In Section IV, we describe the robustness of NF in a 3×3 array with disorder. Finally in Section V, we summarize and discuss essential results about quantum magnetism that can be revealed by simulations done on small arrays of dopants or quantum dots.

II. HUBBARD MODEL

NF occurs for electrons described by the Hubbard model, which takes the form as follows

$$\mathcal{H} = t \sum_{\langle i,j \rangle, \sigma} c_{i,\sigma}^\dagger c_{j,\sigma} + U \sum_i n_{i,\uparrow} n_{i,\downarrow} \quad (1)$$

where t is the hopping between nearest neighbor sites, c^\dagger and c are the creation and annihilation operators, n is the particle number operator, and U is the onsite interaction between spin-up and spin-down electrons. NF is determined by a competition between hopping energy and repulsion, hence the parameter that matters is t/U . Some use the hopping term t with a minus sign, but here we use the convention without a minus sign and allow the value of t to be positive or negative. The sign of t is important because in some systems the Nagaoka theorem can be proved for one sign but not the other. The sign of t can often be changed with a basis change. In particular, the transformation between the signs of t can be done for a bipartite system. In these cases, NF, if it occurs, will occur for both signs of t . The $N \times N$ arrays we study are bipartite lattices.

To find out if a system has NF, it is necessary to determine whether the one-hole ground state has maximum spin. For a finite system like the 2×2 array with 3 electrons, the Hamiltonian is small and the energy spectrum can be calculated directly, as shown in [4]. The energies for the two different total spins, $S = 3/2$ and $S = 1/2$ are plotted against the parameter t/U in Fig. 1a. Both energies are shifted with respect to the energy of the maximum-total-spin state $E_{S=3/2} = -2t$. Below $|t/U| \approx 0.053$, the ground state of the system is the maximum-total-spin $S_{max} = 3/2$ state. In the ferromagnetic ground state, the states with $S = S_{max}$ have a degeneracy of $2S_{max} + 1$. In the 2×2 array with 3 electrons, there are four degenerate s_z states with $s_z = -3/2, -1/2, 1/2, 3/2$. Because the Hubbard Model does not include spin-mixing, it is convenient for the ED to work in s_z subspaces. In our simulation, instead of plotting the ground state energy for each of the total spins, we plot the ground state energy for the different spin- z subspaces as shown in Fig. 1b, and shift them by the energy of the state with maximum s_z $E_{s_z=3/2} = -2t$. Below the transition when the system is in the NF regime, the ground state is 4-fold degenerate. The signature of

NF is when the ground states of the spin- z subspaces become degenerate with each other. This guarantees that the ground state of the system has maximum total-spin.

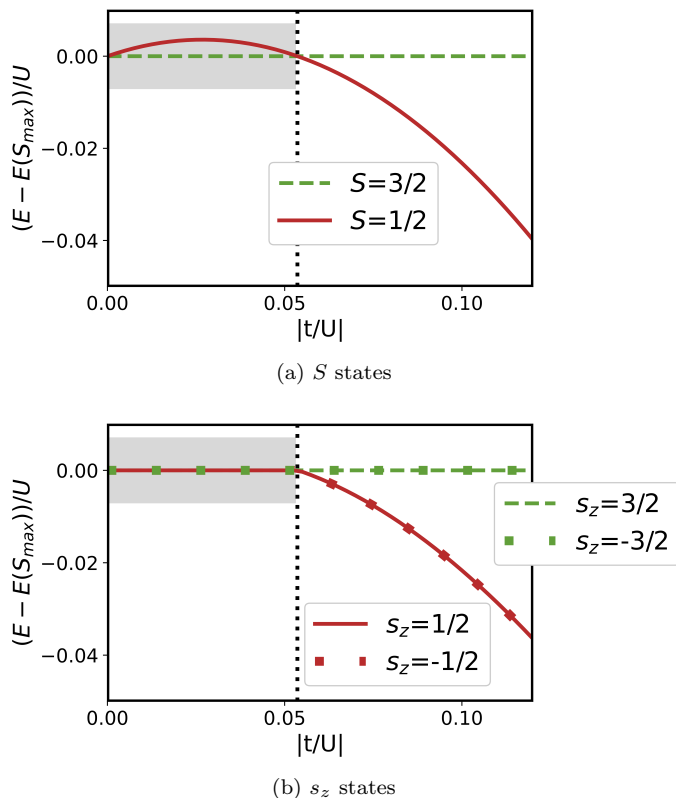


FIG. 1. Nagaoka ferromagnetism in a 2×2 array. (a) Energy spectrum ($S = 3/2$ and $S = 1/2$ as a function of $|t/U|$), which are offset by the energy of $S = 3/2$. Black dotted line indicates the transition for NF. (b) Ground state for each of the different spin z subspaces as a function of $|t/U|$, which are offset by the energy for $s_z = 3/2$. Above and below the transition point, the ground state for $s_z = \pm 1/2$ switches from the total $S = 3/2$ to $S = 1/2$.

Fig. 1 shows how energy behaves as $|t/U|$ varies. The lattice is bipartite so the absolute sign of the t does not matter here, and t and $-t$ give the same energies. This is not always the case as seen later when the system is no longer bipartite, and the $\pm t$ cases can behave very differently. In Fig. 1b, the $s_z = \pm 1/2$ state is always a ground state, but the ground state after the transition has a different total S and degeneracy compared to before the transition. This change in total spin can be verified by direct calculation of the total spin for each spin z .

The NF in 2×2 array has been verified experimentally in [4] for a 2×2 gated quantum dot plaquette. An ab initio calculation of NF in quantum dots was done in [21]. Its robustness was discussed in [21] and theoretically in [13].

III. LARGER SQUARE ARRAYS

A. 3×3 case

The 2×2 array has no internal site. However, the 3×3 dopant array studied by [19] has one internal site. In this section, we look at 3×3 arrays and beyond to see how NF behaves as the size of the system increases and the system approaches the 2D bulk limit. NF has not yet been studied in these larger systems, which should be accessible with dopant arrays. Our results will define the t/U ratios needed for NF. For the 3×3 array, the ground state energy for each spin- z subspace is calculated to determine the presence of NF, and if it exists, to identify the point at which the transition occurs. The half-filled band with one hole has 8 electrons, and the maximum total spin is 4. If all 9 s_z subspaces have the same ground-state energy, the system has NF.

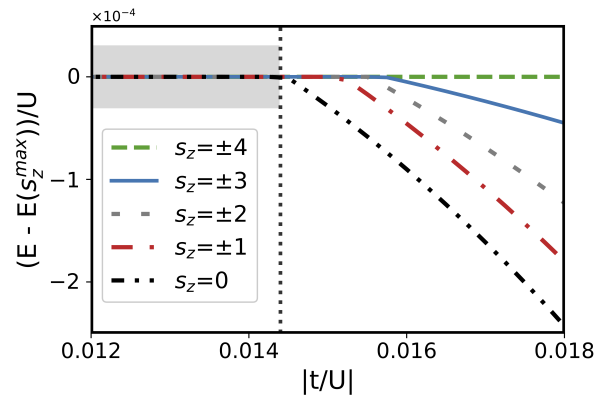


FIG. 2. NF in a 3×3 array. Black dotted line indicates the transition for NF. Ground state for each of the different spin z subspaces plotted as a function of $|t/U|$, which are offset by the energy for $s_z = 4$. When the plotted energy difference for an s_z ground state becomes negative, the total spin of the ground state for that s_z switches from $S_{max} = 4$ to a lower S .

We plot the ground state (GS) energy for each subspace in Fig. 2 (again shifted by the GS energy for maximum s_z). For a small t/U or a large U , the s_z states are all degenerate, i.e. the system has a maximum spin ground state. This is in contrast to the usual anti-ferromagnetic spin order near half-filling, where states have increasing energy as s_z increases. The maximum spin GS holds up to $|t/U| \approx 0.0144$ (black dashed line). After this transition, it becomes higher in energy than the smaller total spin states and is no longer the ground state. Each s_z GS other than the $s_z = 4$ GS has a different total spin below and above the transition.

In the 2×2 array geometry the four sites are equivalent. The 3×3 array geometry is more complicated than the 2×2 geometry because there are three different, inequivalent kinds of sites: the four corner sites are like the 2×2 sites with two connections only to other external sites; the four

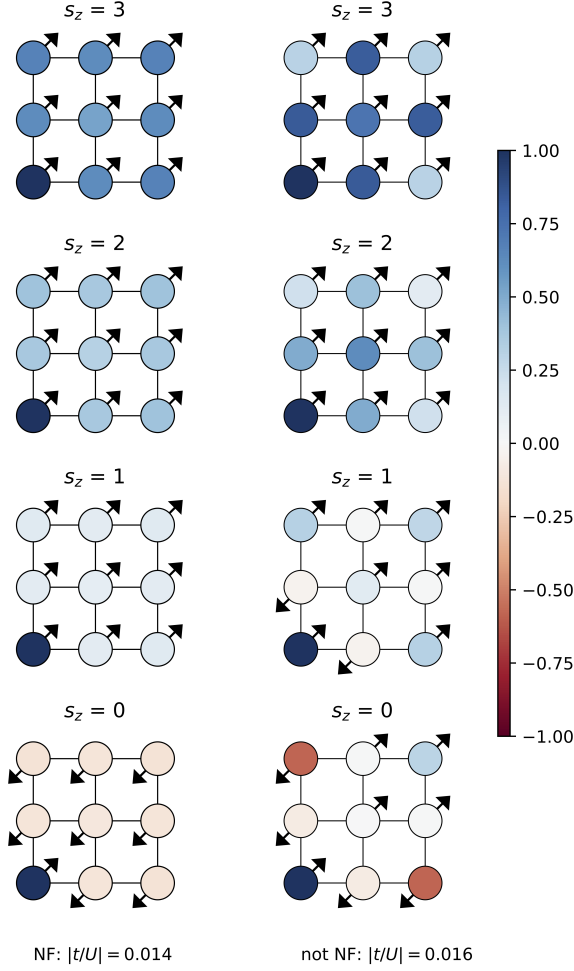


FIG. 3. Ground state correlation function for the 3×3 system below and above the NF transition when the lower-left array-site has a spin-up electron. The correlation function for each non-negative spin- z ($s_z = 3, 2, 1, 0$) ground state is shown. The negative s_z GSs have the same plots but for correlation with a spin-down instead of a spin-up electron. The correlation function ranges from -1 to 1, indicated as the color ranges from dark red to dark blue. The arrow points in the upper right direction when the site is positively correlated, and to the bottom left when it is negatively correlated. In the NF regime, below the transition point, the ground state is ferromagnetic; above the transition, the ground state has a smaller total spin, the correlation plots show quasi-antiferromagnetic characteristics.

edge sites that have one additional hopping to the center site, and one center site that is the only internal site, fully connected with four nearest neighbor hoppings. Despite the more complicated structure, the energies for the s_z GSs for the 3×3 array follows a similar pattern to the GS energies of the 2×2 array, as can be seen by comparing Figs. 1b and 2. The transition is at $|t/U| \approx 0.0144$, which is lower than the transition for the 2×2 array at 0.053, showing that larger interaction is needed for the transition to occur in the 3×3 array.

To see how electrons are organized below and above the transition, we calculate the pair correlation function (CF). The CFs are determined by fixing the number and spin of an electron on one chosen site and calculating the probability of having spin up/down electrons on the other sites. The probability of having spin up is subtracted from the probability for spin down, indicating whether the other site is positively/negatively correlated with the fixed site. The correlation function for a fixed configuration σ_f on site f with some other configuration σ_o on site o is,

$$C_{\sigma_f, \sigma_o} = \frac{\sum \alpha^2[\sigma_f, \sigma_o, \uparrow]}{\sum \alpha^2[\sigma_f]} - \frac{\sum \alpha^2[\sigma_f, \sigma_o, \downarrow]}{\sum \alpha^2[\sigma_f]} \quad (2)$$

where $\sigma_{o, \uparrow/\downarrow}$ indicates the spin up/down occupation of site o , $\alpha[\sigma_f]$ is the probability amplitude for any configuration of site occupations that includes the σ_f occupation, and $\alpha[\sigma_f, \sigma_{o, \uparrow/\downarrow}]$ is the probability amplitude for any configuration that includes the site occupations at f and o . The amplitudes' squared are summed over all configurations with the appropriate site occupations. The correlation function of the s_z GS for the 3×3 array when one spin-up electron is fixed on the corner is plotted in Fig. 3. The color indicates the strength of the correlation, if the other site is dark blue, the density on that site is has more spin-up than spin-down and is positively correlated with the fixed up-spin at the corner site. A dark red site indicates the site has larger spin-down density. The direction of the arrow at each site also shows whether the site is positively or negatively correlated with the spin at the fixed site. Fig.3 compares the correlation function below and above the transition point for $s_z = 3, 2, 1, 0$. Correlations that are ferromagnetic below the transition becomes locally antiferromagnetic above the transition for the small s_z GSs.

From the correlation plots shown in Figs. 3 and 4, the states below and above the transition look qualitatively different because the GS for each spin z switches to a state with the same spin z but smaller total spin S . This is confirmed by following the energies for the first few excited states, which have a different total spin from the ground state. Fig. 4 shows a blow-up of the region near the transition. Below the transition, the ground state energy is the maximum-total-spin state. An excited state below the transition with the same s_z but smaller total S becomes the ground state above the transition. As $|t/U|$ moves away from the transition point, the correlation functions for different total-spin states do not change qualitatively, but vary slowly and continuously across and away from the transition.

Nagaoka ferromagnetism occurs when there is one hole in a half-filled band. We have checked for other fillings. The one-hole case is the only filling that exhibits saturated ferromagnetism with a maximum-total-spin ground state at large enough U .

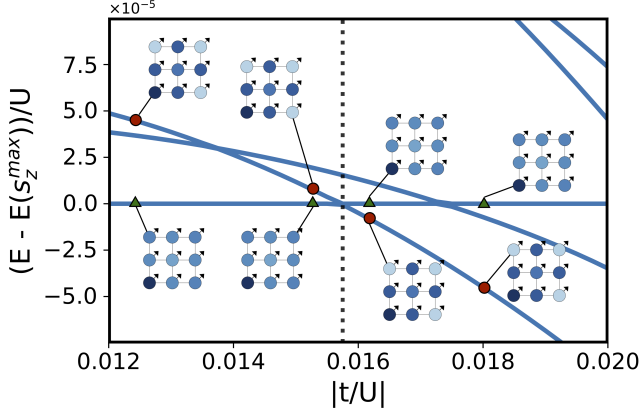


FIG. 4. Correlation function for energies for $s_z = 3$ as a function of $|t/U|$ near the transition point, offset by the maximum-spin-state energy. A spin-up electron is fixed at the lower-left array-site. Correlation plots are displayed at markers. Green triangles indicate a ferromagnetic state, while red circles indicate a state with same $s_z = 3$ but smaller S . The black dotted line is the transition point. Note that for $s_z = 3$ subspace, the transition point is larger at $|t/U| \approx 0.0157$ instead of 0.0144. Markers are t/U values chosen arbitrarily to show how correlation plots change ($|t/U| = 0.0125, 0.0153, 0.0162, 0.018$).

B. $N \times N$ arrays

NF was first predicted for a 2D extended bulk system of electrons with infinite interaction U . The bulk limit should be reached as the size of an $N \times N$ array increases. To see if NF for one hole in a half-filled band still occurs for small t/U as N increases and, if so, how the transition point changes as the array size increases, and to see if ferromagnetism can appear for smaller band fillings for larger N we have studied $N \times N$ arrays for $N = 4, 5, 6$, and 7.

Simulation done for 4×4 and 5×5 arrays for one-hole in a half-filled band are shown in Fig. 5a. The larger $N \times N$ arrays behave similarly to the 3×3 and 2×2 arrays, with the transition point decreasing as N gets larger, as shown in Fig. 5b. As the $N \times N$ array gets larger, the onsite interaction U needs to be larger for NF to occur. This agrees with Nagaoka's original theorem, that ferromagnetism in an infinite lattice occurs for infinite onsite interaction U . Fig. 5a includes the results from ED and DMRG (density matrix renormalization group) simulations. For smaller s_z the large number of possible spin configurations makes ED difficult even for 4×4 and 5×5 arrays. When ED calculations are not possible, we perform DMRG simulations. Here, we flatten the 2D arrays into 1D chains with long-range hoppings, and obtain their ground state energies through the well-established two-site iterative variational searches [22, 23]. The DMRG calculations confirm the prediction that for larger $N \times N$ arrays, NF exists for a smaller region of $|t/U|$. The dependence of the transition ratio on array size N shown

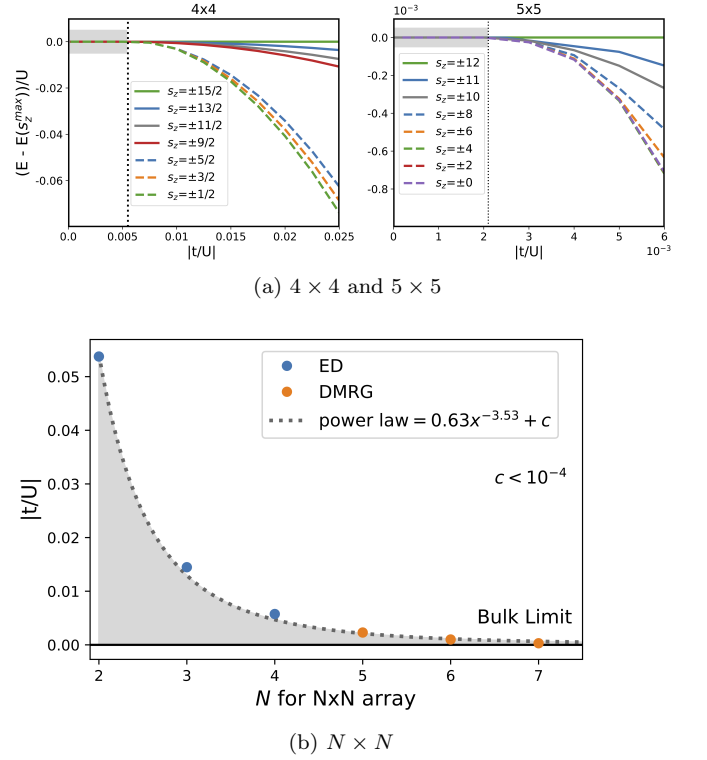


FIG. 5. NF for $N \times N$ arrays. (a) NF for 4×4 and 5×5 arrays. Energy of the ground state for each spin z subspace plotted as a function of $|t/U|$, offset by the energy of the maximum-total-spin state. The black dashed line indicates the transition for NF. Both systems are in the one hole case, with S_{max} for 4×4 arrays $S_{max}^{4 \times 4} = 15/2$, and for 5×5 arrays $S_{max}^{5 \times 5} = 12$. Here only s_z subspaces accessible with ED are shown. (b) Transition point vs N , including both ED and DMRG results. Fitted exponential and power law functions shows how the system approaches the bulk limit (Nagaoka limit $U \rightarrow \infty$) as N gets larger.

in Fig. 5b out to the 7×7 array has been well fitted to both an exponential and inverse power law on N . In the appendix, a scaling argument is used to support an inverse power law dependence on N . The 7×7 is the first lattice with more internal sites than edge sites. Our results suggest that the bulk limit for NF ferromagnetism with U becoming very large is being approached by $N=7$. Table I summarizes the results for $N \times N$ arrays.

IV. ROBUSTNESS OF NF IN 3×3 ARRAYS

In actual experiments with dopant arrays [19], the arrays are not perfectly ordered. Disorder in dopant position and dopant number exists, which can affect the tunnelling and onsite energies. In dopant quantum dot systems intended to have only one dopant at each site, there can be more than one dopant clustered near a site. The properties of that disordered site are determined by the multidopant cluster. This results in a different on-site

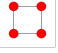
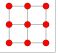
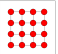
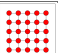
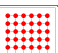
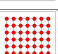
Geometry	Sketch	NF	# of e^-	Transition	Methods
2×2		yes	3	0.053	ED
3×3		yes	8	0.0144	ED
4×4		yes	15	0.0058	ED, DMRG
5×5		yes	24	0.0023	ED, DMRG
6×6		yes	35	0.001	DMRG
7×7		yes	48	0.0003	DMRG

TABLE I. $N \times N$ arrays results: geometry, sketch, whether Nagaoka ferromagnetism exists, number of electrons, and transition point, calculational methods.

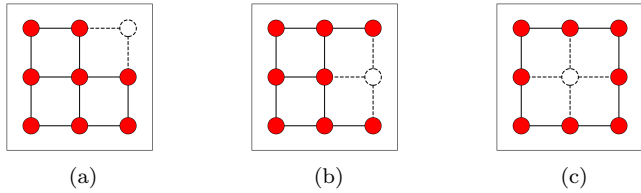


FIG. 6. Three ways of removing one site from a 3×3 array at (a) a corner, (b) an edge and (c) the center.

energy for that particular site compared to the on-site energy that is common to the array sites with a single dopant. It is harder for electrons to hop on and off the disordered site, lowering the participation of that site in the array states. When the energy of the disordered site is sufficiently far off-resonance from the other sites, the disordered site is effectively removed from the array. To investigate the robustness of NF in realistic 3×3 arrays, we consider 3×3 arrays with one site missing to see if ferromagnetism survives or disappears, and, if ferromagnetism survives, what electron fillings display the ferromagnetism. This will provide us insight into how and when NF exists in small finite systems with realistic conditions. For the 3×3 array, there are three different types of site, the corner, edge, and center sites, corresponding to having 2, 3, or 4 hoppings connecting it to other other sites. Removing one site of each type of atom is shown in Fig. 6. We discuss these three cases in the next three sections. We will also discuss ferromagnetism in other finite structures that can be made by removing similar sets of sites in larger $N \times N$ arrays. We summarize the results for removing sites from the 3×3 array and other extended structures in Table II.

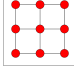
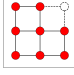
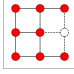
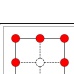
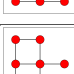

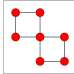
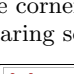
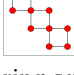
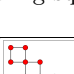
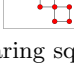
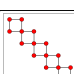

Geometry	Sketch	NF/IF?# e		Transition	Details
3×3		NF	8	0.053	1-hole NF
no corner		NF	7	0.0104	1-hole NF
no edge		no			not connected
no center		IF	3	0.131	$3e$ IF
no same-side corner		no			not connected
no opposite corner (2 corner-sharing sq)		IF	5	0.0127	2-hole IF
3 corner-sharing sq		IF	8	0.0015	2-hole IF
4 corner-sharing sq		IF	11	0.0011	2-hole IF
5 corner-sharing sq		IF	14	0.00022	2-hole IF
2x3 (2 side-sharing sq)		NF	5	0.019	1-hole NF
2x4 (3 side-sharing sq)		NF	7	0.012	1-hole NF
2x5 (4 side-sharing sq)		NF	9	0.0082	1-hole NF
N-site loops		IF	3	$0.017N - 0.002$	$3e$ IF

TABLE II. Summary table for other geometries, their sketch, whether Nagaoka ferromagnetism (NF) or itinerant ferromagnetism (IF) exists, number of electrons, and transition point if applicable.

A. Removing a Corner

We consider first removing one corner atom (shown in Fig. 6a), which removes the fewest hoppings and gives a structure most similar to the original 3×3 array. After one of the corner atoms is removed, the structure becomes three 2×2 squares stacked together, sharing common sides. NF still exists but now for one-hole in the new half-filled band, i.e. now for 7 electrons. The transition point at $|t/U| \approx 0.0104$ is slightly lower than for the full 3×3 array at 0.0144. Removing one site can be modeled by increasing the onsite energy of that site. When the onsite energy is zero (same as the other sites in the array), the system is the full 3×3 array. When the onsite energy is infinite, the array has one less site. In this paper, we have discussed these two limits for the onsite energy of the disordered site. In an upcoming paper, we will show how the ferromagnetism evolves from NF on a 3×3 array to NF on an array with one less corner site and one less electron when the disorder in the site-energy at a corner is increased.

There are two different ways to remove two corner sites in a 3×3 array, as shown in lines 5 and 6 in Table II. If two corner atoms on the same side are removed, the structure becomes a 2×3 rectangle connected by one extra hopping to an edge site. This geometry does not exhibit GS ferromagnetism for one hole in the half-filled band.

Tasaki showed [2] that for NF to exist the many-body wavefunction must satisfy a connectivity condition. Here, being a connected many-body wavefunction requires that each site be connected to other sites in the lattice by hopping and, more importantly, that any configuration of spins in the array can be connected, via hopping without double occupancy, to any other configuration of the same spins in the array. Connectivity is a necessary but not sufficient condition for saturated ferromagnetism. For an array with a hanging single hopping as shown in line 5 of Table II, a spin on the isolated site connected to the rest of the array by one hopping can be moved off the isolated site only by exchanging with a hole on its only neighbor. However, the spin can't be moved further to another site in the array unless a second hole is present. This is shown in Fig. 7a. The many-body wavefunction for this geometry is not connected for one-hole in a half-filled band and can't realize saturated ferromagnetism for that filling. This prohibits NF for one-hole in a half-filled band. However, the many-body wavefunction becomes connected when there are two or more holes in the half-filled band. However, we didn't find GS saturated ferromagnetism for any number of holes. This shows that the connectivity condition is necessary but not sufficient.

If the two sites are removed from opposite corners of the 3×3 array, the structure becomes two 2×2 plaquettes connected by sharing a common corner site. The ground state for this structure is ferromagnetic only when there are two holes in a half-filled band of the array. The transition is at $|t/U| \approx 0.0127$ and calculations of the pair

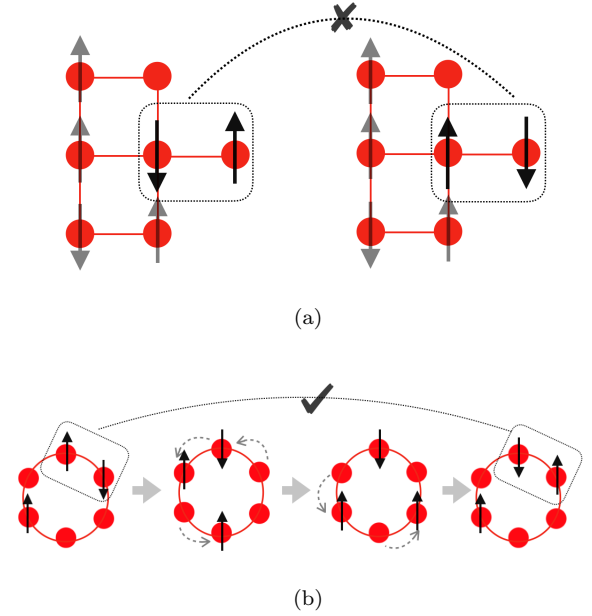


FIG. 7. (a) An example showing when the connectivity condition for NF is violated. To exchange the two spins (in the box), a series of nearest neighbor hoppings is not sufficient, as the spin up and spin down electrons must be on the same site which is strongly suppressed by large repulsion U . (b) Example of the connectivity condition being satisfied for 3 electrons on a loop. For any sized loop, 3 electrons is the only filling where the wavefunction is connected. Any pairs of spins (shown in the box) can be exchanged when the other electrons hopped around the loop.

correlation function show ferromagnetic behaviour below the transition. We refer to this as the itinerant ferromagnetism (IF) case because it is not restricted to the one-hole in a half-filled band of NF. This ferromagnetism for two-holes in a half-filled band can be extended to longer chains of squares. The ground state of the longer chains of corner-sharing squares is ferromagnetic but only when there are two holes in a half-filled band, and not ferromagnetic for the one-hole case (the NF state). The many-body wavefunction is not connected when there is one-hole in a half-filled band, preventing GS saturated ferromagnetism. The site that the two 2×2 plaquettes share acts as a bottleneck. A hole, on one of the 2×2 plaquettes can't be used to move a spin around another plaquette that has spins at each site. A second hole is needed. Hence ferromagnetism is possible for 2 holes, as we have found. As before, this is a necessary but not sufficient condition. Saturated ferromagnetism does not exist for more than two holes. As the chain gets longer, the transition point also decreases as happens when arrays increase in size.

One might think that the 2-hole ferromagnetism occurs when the two holes are localized to the two 2×2 plaquettes at the end of the chain. However, calculations of the local charge density show that the two holes are spread across the entire chain. The two-hole condition appears

to arise primarily from the wavefunction connectivity.

B. Removing an Edge Site

In Fig. 6b, the middle site on an edge is removed. We refer to this removed site as an edge site. This leaves the array with two sites at the corners of the array attached to the 2×3 rectangle by single bonds. For this array, there is no ferromagnetism for any number of holes in the half-filled band, i.e. for any electron filling. As seen for an array with same-side corners removed, the many-body wavefunction is not connected for one-hole in a half-filled band of the array with a missing edge site. Thus, NF is not possible. The many-body wavefunction becomes connected for two holes, but there is still no GS ferromagnetism for any number of holes.

If the single hoppings and the isolated sites are removed, the structure turns into a rectangle with internal side-to-side hoppings, and NF appears again for one hole in the half-filled band of the rectangle. The rectangle can be extended to longer chains of 2×2 plaquettes with each pair of adjacent squares sharing a common side. Again, the transition point decreases as the system gets longer. The results for the rectangles can be seen in line 10 – 12 in Table II.

C. Removing the Center Site

When the center site is removed from the 3×3 array, the array becomes an eight-site loop. The many-body wavefunction for this loop is not connected for one-hole in a half-filled band, as shown by Fig. 7b. As a consequence, NF can't exist. Our calculations confirm this. Interestingly, the 8-site loop does have a ferromagnetic ground state for filling by 3 electrons. This result exists regardless of the size of the loop, and the transition point increases linearly as the number of sites on the loop increases, shown in Fig. 8. In fact, the many-body wavefunction on the loop is connected for a filling of three electrons. The many-body wavefunction is not connected for any higher electron filling. Thus, a ferromagnetic GS should only be possible for a filling of 3 electrons.

The Nagaoka ferromagnetism of $N \times N$ arrays is very different from the GS ferromagnetism of 3-electron N site loops. Nagaoka ferromagnetism in an $N \times N$ array occurs for one-hole in a half-filled band, i.e. for a number of electrons that increases as N increases. The loop ferromagnetism occurs only for 3 electrons, regardless of the number of loop sites N . The transition t/U decreases as an inverse power law of N in $N \times N$ arrays, requiring larger U to achieve ferromagnetism in a larger array. For a loop, the transition point increases linearly with increasing loop size. In the appendix, the inverse power law for $N \times N$ arrays and the linear dependence for loops is explained based on arguments for how the hopping energy and the repulsive energy of interaction scale with

system size. The opposite scaling behavior is related to how the hopping energy scales in $N \times N$ arrays with an almost half-filled band and in loops filled with only 3 electrons with system size. The t/U transition ratio for NF in 2×2 arrays is 0.05 and is smaller for larger arrays. The hopping t is much smaller than U at the transition point for all square arrays. The transition point for itinerant ferromagnetism in loops quickly becomes of order 1 with t similar to U , as the loop size increases, for all but the smaller loops. The 2×2 array can also be thought as a 4-site loop. In this case, one-hole in a half-filled band is three electrons, so the filling for ferromagnetism is the same whether the array is considered a 2×2 array or a 4-site loop. There is ambiguity in whether ferromagnetism should be considered Nagaoka ferromagnetism or 3-electron loop ferromagnetism. For larger systems this distinction becomes clear.

The specific cases for pentagons and hexagons were discussed in [14], which described a pattern of ferromagnetism appearing in small pentagonal and hexagonal plaquettes at filling factors of roughly $3/10$ and $1/4$. However, this density dependence appears to be an artifact due to the different geometries considered. In each case, the ferromagnetism occurs for 3 electron filling. This is not a density effect. This filling for ferromagnetism arises because 3-electron filling is the only filling on loops that allow a connected many-body wavefunction.

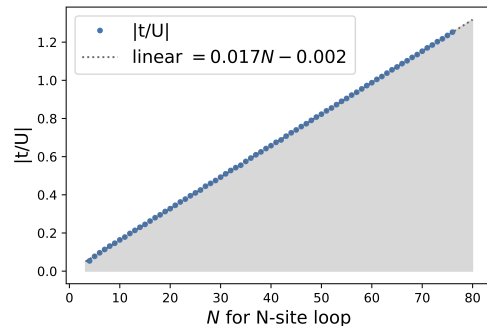


FIG. 8. Dependence of the transition point $|t/U|$ on loop size. As the loop gets larger, the transition point gets larger. Here only loop sizes accessible with ED are shown. Linear fit is shown.

When the loop sites are arranged evenly on a circle, each site position can be parameterized by an angle ϕ with $0 \leq \phi \leq 2\pi$. Fixing one site on the loop at $\phi = 0$, the correlation functions (CF) for the remaining electrons can be plotted against the angle. In Fig. 9, the CFs for a fixed spin up $CF(\uparrow)$ and spin down $CF(\downarrow)$ for three electrons on loops of various sizes are plotted against angle in the first and second columns. Here we display a GS when $s_z = 1/2$. When system is in the IF regime for small t/U ratio, the spin up/down CFs have peaks at angles $\phi = 2\pi/3$ and $4\pi/3$, with the electrons as far away from each other as possible, and with a total spin of the ground state that is maximum at $S = 3/2$. $CF(\uparrow)$ and $CF(\downarrow)$ are the same, showing that the two other elec-

trons, regardless of spin, are correlated the same way to the fixed spin, as would be expected when interaction is dominant. After the transition when the t/U ratio is large, the saturated ferromagnetism is lost, the two-peak structure disappears, the electrons behave qualitatively differently and the GS is no longer the maximum total spin. For a fixed spin-up electron, the other two electrons are spin up and spin down. With weak correlation, the other spin-up electron stays as far away as possible from the fixed spin-up electron. In contrast, when the spin-down electron is fixed, the remaining two electrons are spread almost uniformly around the entire ring with little correlation as expected when hopping is dominant.

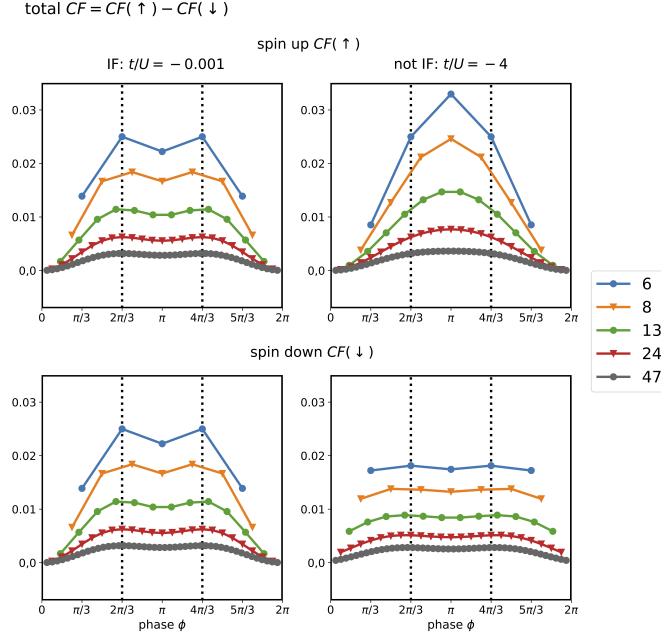


FIG. 9. Dependence of the spin-up and spin-down correlation functions vs. angle for a loop with three electrons, $s_z = 1/2$ and spin-up electron fixed at $\phi = 0$. Different loop lengths are shown. The left column is for an IF GS below t/U transition. The right column is for a GS above the transition where there is no IF.

Note, the sign of t matters for loops. For odd-numbered loops, the ferromagnetism for 3 electrons only occurs when $t < 0$. There is no ferromagnetism for $t > 0$ for any filling. For even numbered loops, the ferromagnetism for 3 electrons exists regardless of the sign of t . The even-numbered loops are bipartite and a transformation between t and $-t$ can be done.

V. SUMMARY AND DISCUSSION

In this work we have presented theoretical simulations done to probe Nagaoka ferromagnetism in arrays with different geometries. Starting from the 2×2 plaquette, which was experimentally realized in [4], we have shown that perfect 3×3 and $N \times N$ arrays up to 7×7 exhibit

NF for one-hole in a half-filled band, with a t/U ratio for the onset of NF that decreases as the array size N increases. So far 2D dopant arrays have only been studied for the 3×3 configuration. However, recent advances in fabrication of dopant structures gives significant promise for making highly engineered dopant arrays that will be an excellent testbed as an analog quantum simulator for this quantum magnetism.

The existence of Nagaoka ferromagnetism or other forms of itinerant ferromagnetism crucially depends on the system geometry. One of the geometrical, necessary criteria is connectivity, not only in physical space, but also in the many-body spin-configuration space, which requires that any configuration of spins in the array can be transformed to any other configuration by a series of nearest neighbor hoppings without double occupancy. In $N \times N$ arrays, at least one hole is needed in a half-filled band for wavefunction connectivity at that filling. The $N \times N$ array has saturated ferromagnetism at this filling. A chain of 2×2 square plaquettes with adjacent plaquettes connected at a common corner need at least two holes in a half-filled band to support wavefunction connectivity and supports saturated ferromagnetism for small t/U . In contrast, N site loops have wavefunction connectivity only for three-electron filling and saturated ferromagnetism for this filling.

A simple scaling argument shows that kinetic energy plays a critical role in determining the size dependence of the t/U ratio at the onset of saturated ferromagnetism. In quasi two-dimensional systems, such as $N \times N$ arrays and chains of 2×2 plaquettes, with ferromagnetism near half-filling, the critical t/U decreases as the system size increases. A smaller hopping t is needed to suppress ferromagnetism in larger systems because the kinetic energy increases more quickly than the repulsive energy as the size increases. In one-dimensional, N -site loops, with saturated ferromagnetism only for three electron filling, the critical t/U increases as the loop size N increases and ferromagnetism can occur for larger t and N increases. The scaling argument for small filling shows that the kinetic energy contribution becomes less important for larger loops, allowing the ferromagnetism to persist.

The robustness of the saturated ferromagnetism to disorder in $N \times N$ arrays has been tested by considering 3×3 arrays with one site removed. When a corner site is removed, saturated ferromagnetism is still possible for one hole in a half-filled band (which now has one less electron). When one of the edge sites is removed from the 3×3 array saturated ferromagnetism is no longer possible because wavefunction connectivity is broken. When the center site is removed, the 3×3 array becomes a loop. Saturated ferromagnetism is still possible but only for three electron filling, which is the only filling that has wavefunction connectivity. The transition between different realizations of ferromagnetism when a site is removed can be mapped out by varying the on-site energy of the site to be removed. The phase diagrams associated with these transitions will be discussed in a future

publication.

Interestingly, the first experiment to demonstrate Nagaoka ferromagnetism was for a 2×2 plaquette. The 2×2 plaquette is the smallest $N \times N$ array where one hole in a half filled band requires three electrons. However the 2×2 array is also a loop that displays the three-electron ferromagnetism expected for loops. It is not clear whether ferromagnetism in 2×2 plaquettes is best described as Nagaoka ferromagnetism or as three-electron loop ferromagnetism.

Our results show that many forms of ferromagnetism are possible in complex, extended arrays. Both small-scale and extended dopant arrays should be a rich playground to explore quantum magnetism.

ACKNOWLEDGMENTS

This material is based upon work supported by the National Science Foundation under Grant No 2240377.

Appendix A: Scaling of the transition ratio with system size

There are two dramatic differences between Nagaoka ferromagnetism in $N \times N$ arrays and three-electron ferromagnetism in N -site loops. First, the band-filling necessary for saturated magnetism is related to the many-body wave function connectivity, which, in turn, is related to the system geometry. The geometries of the $N \times N$ array and the N -site are very different, leading to very different criteria for wave function connectivity. Nagaoka ferromagnetism in an $N \times N$ array occurs when there is one hole in a half-filled band. The number of electrons involved is $N \times N - 1$. Three-electron ferromagnetism occurs in loops for three-electron filling, independent of loop size.

The second essential difference is the scaling of the t/U ratio at the ferromagnetic transition with the system size N . For $N \times N$ arrays, the t/U ratio at the transition scales as $1/N^3$, as shown in Fig. 5b. As the array size N increases, a larger U is needed to transition to ferromagnetism, making it harder to reach ferromagnetism as N increases. For N -site loops, Fig. 8 shows that the t/U ratio at the transition scales as N . As the loop size increases, a smaller U is needed for the transition to ferromagnetism, making it easier to for this transition to take place.

In this appendix we show how this dramatic difference in scaling can be understood based on simple arguments about how the difference in system hopping energy $\Delta T_{sys}(N)$ before and after the ferromagnetic transition and the corresponding difference in system electron-electron repulsion $\Delta U_{sys}(N)$ scale with the system size. To make the scaling argument, we assume that there is a critical ratio R_{crit}^{sys} for $\Delta T_{sys}(N)/\Delta U_{sys}(N)$ that determines the relative strength of the hopping and interaction

energies needed for the transition to ferromagnetism. We assume that R_{crit}^{sys} may be different for loops and arrays, but does not depend on N . The usefulness of these two assumptions will be supported by the scaling relations that can be derived and by the success of the derived relations in explaining the opposite scaling with N for loops and arrays.

1. Scaling of the number of participating electrons

For the $N \times N$ array with one hole in a half-filled band, the number of electrons contributing to the total hopping energy scales as N^2 . The number of electron pairs contributing to the interaction energy scales as N^4 . For the N -site loop the scaling is very different. For the three-electron ferromagnetism, three electrons contribute to the hopping energy, independent of loop size. At most six electron-pairs contribute to the interaction energy, independent of loop size. This very different scaling for arrays and loops will explain most of the very different scaling for the t/U ratio.

2. Scaling of the hopping energy difference

The transition to saturated ferromagnetism occurs once each ground state for total s_z becomes the s_z -state with maximum total S . As shown in Figs. 2 and 5a, the ground state with maximum polarization transitions to the state with maximum S at higher t/U and the ground state with minimum polarization transitions to the state with maximum S last as t/U is decrease. To estimate the scaling for the hopping energy difference we consider the transition of state with minimum polarization. This state will have nearly an equal number of up and down spins. For a nearly half-full band, the Fermi level for each spin will be at the middle of the band. States that can be rearranged in the ferromagnetic transition will be close to the middle of the band. The bandwidth of hopping energy in the array scales as t . There are N^2 states in the band for each spin. These states should have hopping energies that scale as t/N^2 , especially near the band center. The number of electrons contributing to the transition should scale as N^2 . The change in hopping energy of the array with one hole in a half-filled band should be independent of N .

For the loop, only three electrons contribute to the change in hopping energy and these states have hopping energies near the band edge, which scales as t . The total hopping energy for a filling with three electrons should scale as t .

3. Scaling of the interaction energy

The easiest way to establish the scaling is to consider the continuum limit for the array as a square hard-wall

box. The interaction energy of a pair of electrons of opposite spin should be proportional to U and the probability that the two spins overlap. In one dimension of the box, the probability that two plane-wave single-particle states overlap should scale as $1/L$ where L is the length of the box side and L scales as N . The probability of overlap for the square box will scale as $1/L^2$ when both dimensions are accounted for. The interaction per opposite-spin pair will scale as U/L^2 and the change in interaction energy $\Delta U_{array}(N)$ will scale as UN^2 , where the number of opposite-spin pairs near the Fermi level scales as N^4 .

For the loop, similar arguments show that the overlap along the loop scales as $1/L$. Unlike the square array, the loop is one dimensional so the scaling factor for the overlap differs for loops and arrays. The change in interaction energy per pair scales as U/L and the total interaction energy for three electrons on the loop scales as U/N .

4. Scaling of the ratio $T_{sys}(N)/U_{sys}(N)$

Using the scaling relations for the change in hopping energy and the change in interaction energy for the array, the critical ratio for the array should scale as

$$\Delta T_{array}(N)/\Delta U_{array}(N) \sim t/(UN^2).$$

As a result, the t/U ratio at the ferromagnetic transition for the array with one-hole in the half-filled band should

scale as

$$t/U \sim R_{crit}^{array} N^2.$$

Using the scaling relations for the change in hopping energy and the change in interaction energy for the loop, the critical ratio for the loop should scale as

$$\Delta T_{loop}(N)/\Delta U_{loop}(N) \sim (t)/(U/N).$$

As a result, the t/U ratio at the ferromagnetic transition for the loop with three electrons should scale as

$$t/U \sim R_{crit}^{loop}/N.$$

Most importantly, the scaling relations for t/U show and explain the opposite behaviour for loops and arrays. For loops, t/U scales inversely with N just as our numerical results show. In contrast, for arrays the scaling relation predicts quadratic scaling with N , slower scaling than the N^3 scaling in the numerical results. Three factors contribute to the different scaling. Most importantly, electrons near the middle of band contribute to the scaling for arrays. For loops, only a three electrons near the band edge contribute. For arrays there are extra factors of N^2 and N^4 that determine the scaling of hopping and interaction energy, For arrays, the hopping energy for electrons near the middle of the band has a $1/N^2$ scaling, while for loops, the hopping energy of three electrons near the band edge scales independently on N . Finally, the interaction energy per pair scales as $1/N^4$ in two-dimensional arrays, as compared to the $1/N^2$ scaling in one-dimensional loops.

-
- [1] Y. Nagaoka, Ferromagnetism in a narrow, almost half-filled s band, *Phys. Rev.* **147**, 392 (1966).
 - [2] H. Tasaki, From Nagaoka's ferromagnetism to flat-band ferromagnetism and beyond: An introduction to ferromagnetism in the Hubbard model, *Progress of Theoretical Physics* **99**, 489 (1998).
 - [3] E. H. Lieb, Two theorems on the Hubbard model, *Phys. Rev. Lett.* **62**, 1201 (1989).
 - [4] J. Dehollain, U. Mukhopadhyay, V. Michal, *et al.*, Nagaoka ferromagnetism observed in a quantum dot plaquette, *Nature* **579**, 528 (2020).
 - [5] A. Mielke, Stability of ferromagnetism in Hubbard models with degenerate single-particle ground states, *Journal of Physics A: Mathematical and General* **32**, 8411 (1999).
 - [6] T. E. Hanisch, B. Kleine, A. Ritzl, and E. Mueller-Hartmann, Ferromagnetism in the Hubbard model: instability of the Nagaoka state on the triangular, honeycomb and kagome lattices, *Annalen der Physik* **507**, 303 (1995).
 - [7] A. Barbieri, J. A. Riera, and A. P. Young, Stability of the saturated ferromagnetic state in the one-band Hubbard model, *Phys. Rev. B* **41**, 11697 (1990).
 - [8] A. Sütő, Absence of highest-spin ground states in the Hubbard model, *Communications in Mathematical Physics* **140**, 43 (1991).
 - [9] B. Tóth, Failure of saturated ferromagnetism for the Hubbard model with two holes, *Letters in Mathematical Physics* **22**, 321 (1991).
 - [10] B. Douçot and X. G. Wen, Instability of the Nagaoka state with more than one hole, *Phys. Rev. B* **40**, 2719 (1989).
 - [11] S. Yun, W. Dobrutz, H. Luo, V. Katukuri, N. Liebermann, and A. Alavi, Ferromagnetic domains in the large- u Hubbard model with a few holes: A full configuration interaction quantum monte carlo study, *Phys. Rev. B* **107**, 064405 (2023).
 - [12] S. Yun, W. Dobrutz, H. Luo, and A. Alavi, Benchmark study of Nagaoka ferromagnetism by spin-adapted full configuration interaction quantum monte carlo, *Phys. Rev. B* **104**, 235102 (2021).
 - [13] D. Buterakos and S. Das Sarma, Ferromagnetism in quantum dot plaquettes, *Phys. Rev. B* **100**, 224421 (2019).
 - [14] D. Buterakos and S. Das Sarma, Certain exact many-body results for Hubbard model ground states testable in small quantum dot arrays, *Phys. Rev. B* **107**, 014403 (2023).
 - [15] T. Hensgens, T. Fujita, L. Janssen, G. Tosi, M. T.

- Rakher, Y. Cao, C. J. Van Diepen, C. Reichl, W. Wegscheider, and L. M. Vandersypen, Quantum simulation of a Fermi-Hubbard model using a semiconductor quantum dot array, *Nature* **548**, 70 (2017).
- [16] P. Barthelemy and L. Vandersypen, Quantum dot systems: a versatile platform for quantum simulations, *Annalen der Physik* **525**, 808 (2013).
- [17] J. Salfi, J. A. Mol, R. Rahman, G. Klimeck, M. Y. Simmons, and L. C. Hollenberg, Quantum simulation of the Hubbard model with dopant atoms in silicon, *Nature Communications* **7**, 11342 (2016).
- [18] J. I. Cirac and P. Zoller, Goals and opportunities in quantum simulation, *Nature Physics* **8**, 264 (2012).
- [19] X. Wang, E. Khatami, F. Fei, and et al., Experimental realization of an extended Fermi-Hubbard model using a 2d lattice of dopant-based quantum dots, *Nature Communications* **13**, 6824 (2022).
- [20] J. Wyrick, X. Wang, P. Namboodiri, R. V. Kashid, F. Fei, J. Fox, and R. Silver, Enhanced atomic precision fabrication by adsorption of phosphine into engineered dangling bonds on h-si using stm and dft, *ACS Nano* **16**, 19114 (2022), pMID: 36317737, <https://doi.org/10.1021/acsnano.2c08162>.
- [21] Y. Wang, J. P. Dehollain, F. Liu, U. Mukhopadhyay, M. S. Rudner, L. M. K. Vandersypen, and E. Demler, Ab initio exact diagonalization simulation of the Nagaoka transition in quantum dots, *Phys. Rev. B* **100**, 155133 (2019).
- [22] M. Fishman, S. R. White, and E. M. Stoudenmire, The ITensor Software Library for Tensor Network Calculations, *SciPost Phys. Codebases* , 4 (2022).
- [23] M. Fishman, S. R. White, and E. M. Stoudenmire, Codebase release 0.3 for ITensor, *SciPost Phys. Codebases* , 4 (2022).